

Strong-coupling QED in a sphere: Degeneracy effects

Daan Lenstra,^{1,*} Gershon Kurizki,^{2,†} Lissette D. Bakalis,¹ and Konrad Banaszek^{1,‡}

¹*Department of Physics and Astronomy, Vrije Universiteit De Boelelaan 1081, 1081 HV, Amsterdam, The Netherlands*

²*Department of Chemical Physics, Weizmann Institute of Science, 76 100 Rehovot, Israel*

(Received 29 March 1996)

We investigate the resonant interaction of a dipolar $j=0 \leftrightarrow j=1$ angular-momentum transition with the quantized field in a dielectric sphere. New features arise on account of the degeneracy of atomic levels and field modes with low azimuthal angular momentum, in slightly deformed spheres (oblate spheroids). For TE-mode excitation we obtain the dynamics of a degenerate Λ or V configuration with the usual coherent-state collapse and revivals. For TM-mode excitation new behavior is found: due to interference between σ - and π -polarized transitions, which can be *controlled* by the atomic position and/or dipole orientation, coherent-state revivals and the corresponding atom-field energy exchange may be suppressed or delayed. [S1050-2947(96)00210-7]

PACS number(s): 42.50.Md, 32.80.Qk, 42.50.Dv, 12.20.-m

I. INTRODUCTION

The realization of the strong-coupling regime of cavity quantum electrodynamics (QED) is currently pursued for atoms or excitons in resonator structures with optical-wavelength dimensions [1–6]. This regime is described in its simplest form by the fundamental Jaynes-Cummings (JC) model [4,5,7], which pertains to the near-resonant interaction of a two-level atom with a single field mode in the rotating-wave approximation (RWA). The JC model yields several important nonclassical effects, such as spontaneous collapses and revivals of Rabi oscillations [7], near disentanglement of field and atom states [8], and generation of Fock states [9–11], or superpositions thereof [11,12] following measurements of the atomic excitation. Other strong-coupling situations are described by the extension of the JC model to the case of two interfering field modes coupled to three-level atoms [13]. Currently most of the aforementioned effects are observable only in extremely high- Q microwave cavities [1,4,5].

Among the resonator configurations that may lead to the realization of strong-coupling QED effects in the optical domain, *spherical microcavities* are particularly promising and important for the following reasons:

- (a) The ability of dielectric microspheres to act as high-quality optical resonators has been proven in a variety of experiments [14], which have indicated sufficiently long mode lifetimes (Q values up to 10^9) to allow the observation of strong-coupling QED in the microsphere, with negligible dissipative effects (well within the mode lifetime).
- (b) The evanescent tail of a high- Q field mode in a dielectric microsphere can be selectively and strongly coupled to a resonance of an atom located up to few

wavelengths outside the surface [15]. Hence, strong-coupling QED effects should be observable in an atomic beam passing near a microsphere. Such effects can be augmented by binding cold atoms in an orbit around a dielectric microsphere via an off-resonant two-photon interaction with its field [16].

- (c) From the conceptual point of view, both classical and QED nonlinear processes in dielectric microspheres are intriguing because of their unique features: (i) the spherical symmetry, which implies *mode degeneracy* and angular-momentum conservation; (ii) the inseparability of the optical fields inside and outside the sphere (leaky modes) [17–19].

The purpose of this paper is to investigate the effects of polarization and degeneracy of spherical modes and atomic levels on the dynamics in the fundamental JC model [4,5,7]. We thereby wish to gain insight into the novel domain of strong coupling of near-resonant atoms with high- Q field modes in microspheres. Field leakage (dissipation) effects will be neglected. Specifically, we study the relatively simple yet nontrivial interaction of $j=0 \leftrightarrow j=1$ atomic transitions with a degenerate multiplet of angular-momentum eigenmodes of the field in a dielectric microsphere, or a spherical cavity. We address the problem of inevitable weak deviations from a perfect sphere, which partly lift the mode degeneracy but still allow the study of degeneracy effects under experimentally realizable conditions.

In Sec. II we discuss the coupling of the $j=0 \leftrightarrow j=1$ transition to either a TE- or TM-polarized degenerate mode multiplet. In Sec. III we diagonalize the interaction Hamiltonian in each such multiplet and obtain the corresponding “dark” (trapping) states of the evolution. In Sec. IV we analyze the generalized Rabi oscillations for photon-number states in both multiplets. In Sec. V we consider the collapse and revivals of these oscillations driven by multimode coherent fields. The main results of our treatment, summarized in Sec. VI, are as follows: (i) trapping conditions for linear combinations of degenerate excited states, which amount to conditions for suppression of the energy exchange with the

*Electronic address: lenstra@nat.vu.nl

†Electronic address: cfkurizk@weizmann.weizmann.ac.il

‡Permanent address: Institute of Theoretical Physics, Warsaw University, Hoza 69, 00-681 Warsaw, Poland.

field, for superposed photon-number and coherent states in the degenerate modes; (ii) conditions for suppression or delay of the first revival of Rabi oscillations, driven by superposed degenerate-mode coherent states. The second effect is akin to that caused by two-mode interference in Raman-like intracavity processes [20]. The present results indicate the possibility of achieving a great deal of control over the atomic and energy-exchange dynamics in a sphere by choosing the appropriate elliptic polarization of the field or the atomic state.

II. THE MODES AND FIELD-ATOM INTERACTION

In this section we analyze the coupling of a $j=0 \leftrightarrow j=1$ dipole transition to the electromagnetic modes in closed spherical cavities with radially varying permittivity $\epsilon(r)$, as well as to the ‘‘quasimodes’’ in open (leaky) dielectric microspheres. We must distinguish between the TE modes, which have the electric-field vector in the tangential direction ($\mathbf{E} \perp \mathbf{r}$) and the TM modes, which have the magnetic-field vector in the tangential direction ($\mathbf{B} \perp \mathbf{r}$). In general, the TE and TM modes have no common frequencies. Both types of modes can be further classified according to the angular-momentum quantum number l , which corresponds to a $(2l+1)$ -fold degenerate multiplet. In addition to the polarization (TE or TM), l and m , the modes are classified according to their index n , which measures the number of *radial* nodes of the field. Low- l modes couple mainly to atoms close to $r=0$. We are primarily interested in high- l modes in spheres whose radius is much larger than an optical wavelength, since these modes couple predominantly to atoms close to the sphere surface [14]. The azimuthal mode number m can be specified as the projection of the angular momentum on the z axis. Hence, the mode m is spatially confined to a great circle, which is inclined at $\theta = \cos^{-1}(m/l)$ relative to z . In an ideal sphere all m modes with given l , n , and polarization (TM or TE) are degenerate. In reality, however, this degeneracy is always lifted to some extent due to distortions that result in a spheroidal shape, which, for the sake of concreteness, is taken here as oblate. This distortion splits the $(2l+1)$ -degenerate modes from the resonance frequency ω_λ ($\lambda = l, n, \beta$, where $\beta = \text{TM or TE}$) of an ideal-sphere mode into a manifold of m -dependent frequencies $\omega_\lambda(m)$. For a small eccentricity ϵ , which is the fractional difference of the polar and equatorial radii, and $l \gg 1$, these m -dependent frequencies are given approximately by [21] $\omega_\lambda(m) = \omega_\lambda \{1 + (\epsilon/6)[3m^2/l(l+1) - 1]\}$. The fractional splitting $\omega_\lambda(m)/\omega_\lambda$ is independent of the polarization (TE or TM), the radial order n , and the radius.

It is possible to selectively populate only a few m modes out of the $(2l+1)$ -fold multiplet by using the spatial confinement of the different m modes [Fig. 1(a)] and the m^2 scaling of their splitting. For nonzero eccentricity, the atom will be chosen to lie near the polar axis of the oblate spheroid. Such an atom can interact with all l modes, but predominantly with $m = \pm 1$ for TE modes and $m = 0, \pm 1$ for TM modes [Fig. 1(b)]. These three modes will be treated as *degenerate*, on the assumption that the splitting $|\omega_\lambda(m=0) - \omega_\lambda(m=\pm 1)| \approx \omega_\lambda \epsilon / 2l(l+1)$ is well below both the atomic and the mode linewidths. As an example, for $\epsilon \leq 10^{-4}$ and surface modes with $l \sim 10^3$, this splitting is $\leq 10^{-10} \omega_\lambda$. In

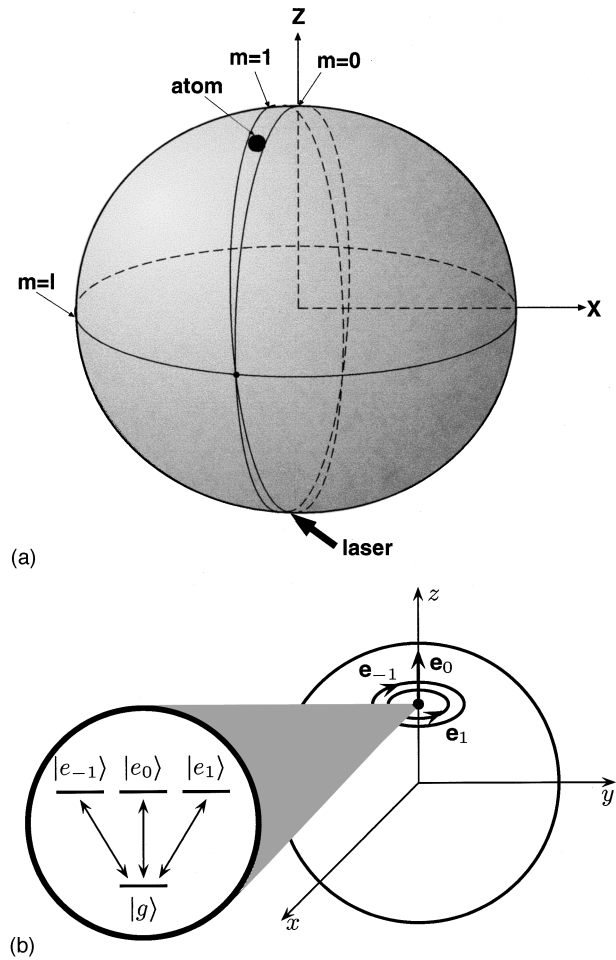


FIG. 1. (a) Atomic coupling to $m=0, \pm 1$ modes at the spheroidal surface. The modes can be externally excited. (b) The coupling of atomic $j=0 \leftrightarrow j=1$ transitions to the electric field at the microsphere surface: the π -polarized transition ($|g\rangle \leftrightarrow |e_0\rangle$) couples only to the radially polarized TM mode ($m=0$), whereas the σ -polarized transition ($|g\rangle \leftrightarrow |e_{\pm 1}\rangle$) couples to both TE and TM tangentially polarized modes ($m=\pm 1$). Inset: The levels corresponding to the above degenerate transitions.

the case of an ideal-sphere cavity, we shall also restrict our treatment to $m=0, \pm 1$, by considering an atom *near* the sphere center, which is resonant with the $l=1$ multiplet.

In either case, as the $\Delta m_j = 0$ (π -polarized) atomic transition implies a radially polarized ($\parallel z$ axis) electric field, it cannot couple to the TE mode. Hence, only the σ -polarized transitions with $\Delta m_j = \pm 1$ couple to the $m = \pm 1$ TE modes, defining a Λ (or V) degenerate configuration [Fig. 1(b)]. By contrast, a TM mode couples to both σ - and π -polarized transitions, and therefore gives rise to two *coupled* Λ (or V) systems.

The corresponding field-atom interaction Hamiltonian can be written in the rotating-wave approximation as

$$\mathcal{H}_{\text{int}} = \hbar d \sum_{\lambda} a_{\lambda} \chi_{\lambda} \cdot \mathbf{\Pi}_{+\lambda} + \text{H.c.} \quad (1)$$

Here the mode indices are denoted by $\lambda = \{\beta; l, m, n\}$ with $\beta = \text{TE or TM}$, a_{λ} is the λ -mode annihilation operator satis-

fying the commutation relation $[a_\lambda, a_\lambda^\dagger] = \delta_{\lambda,\lambda'}$, d is the dipole moment, $\mathbf{\Pi}_{+\lambda}$ is the appropriate dipolar raising operator, and

$$\chi_\lambda(\mathbf{r}) = \begin{cases} R_{l,n}^{\text{TE}}(r) \hat{\mathbf{L}} Y_l^m(\theta, \varphi), & \beta = \text{TE} \\ (ic/\omega_\lambda) \nabla \times R_{l,n}^{\text{TM}}(r) \hat{\mathbf{L}} Y_l^m(\theta, \varphi), & \beta = \text{TM} \end{cases} \quad (2)$$

are the mode eigenfunctions. Here the functions R_{ln}^β are real solutions of the radial wave equation

$$\left[\frac{1}{r^2} \frac{\partial}{\partial r} \left(r^2 \frac{\partial}{\partial r} \right) + k^2 \epsilon(r) - \frac{l(l+1)}{r^2} \right] R_l(r) = 0, \quad (3)$$

Y_l^m are the spherical harmonics, and $\hat{\mathbf{L}}$ is the angular momentum operator. It should be stressed that for small eccentricities ($\epsilon \lesssim 10^{-4}$), the radial character of $R_l(r)$ is practically the same as in an ideal sphere.

In particular, the TE modes with $l=1$ can be expressed as

$$\begin{aligned} \chi_{\pm 1}^{\text{TE}}(r) &= \mp i\sqrt{2}\omega R_1^{\text{TE}}(r) \hat{\mathbf{e}}_{\pm 1}, \\ \chi_0^{\text{TE}}(r) &= 0 \end{aligned} \quad (4)$$

and the $l=1$ TM modes can be expressed as

$$\begin{aligned} \chi_{\pm 1}^{\text{TM}}(r) &= \pm \frac{(-\sqrt{2}c)}{r} \frac{\partial}{\partial r} [r R_1^{\text{TM}}(r)] \hat{\mathbf{e}}_{\pm 1}, \\ \chi_0^{\text{TM}}(r) &= \frac{-2\sqrt{2}c}{r} R_1^{\text{TM}}(r) \hat{\mathbf{e}}_0, \end{aligned} \quad (5)$$

where the unit-vector components are $\hat{\mathbf{e}}_{\pm 1} = 2^{-1/2}(\hat{\mathbf{x}} \pm i\hat{\mathbf{y}})$, $\hat{\mathbf{e}}_0 = \hat{\mathbf{z}}$.

In perfectly reflecting spherical cavities, the normalization of the χ_λ functions is such that

$$\begin{aligned} \int d^3r \epsilon(r) \chi_\lambda \cdot \chi_{\lambda'}^* &= \delta_{\lambda,\lambda'}, \\ \int d^3r (\nabla \times \chi_\lambda) \cdot (\nabla \times \chi_{\lambda'}^*) &= \frac{\omega_\lambda^2}{c^2} \delta_{\lambda,\lambda'}. \end{aligned} \quad (6)$$

In open (leaky) dielectric spheres, there are distinct Mie resonances labeled (β, l, n) , with $l \gg 1$, corresponding to high- Q ‘‘quasimodes’’ localized near the sphere surface with evanescent ‘‘tails’’ outside [14(a)]. A rigorous quantization procedure for such ‘‘quasimodes’’ [14(b)] shows that they can be effectively treated as nearly discrete, *broadened* $(2l+1)$ -degenerate mode multiplets, if the atom is on or just

outside the surface. The radial wave function outside the dielectric sphere is given by the outgoing spherical Hankel function h_l [14],

$$R_{kl}^\beta(r) = C h_l^{(1)}(k_{ln} r), \quad (7)$$

where $\beta = \text{TM}$ or TE , C is the normalization constant, and k_{ln} belongs to a discrete set of wave numbers (Mie resonances). We reiterate that for very small eccentricities, $h_l^{(1)}$ is nearly identical with the spheroidal eigenfunction $h_{le}^{(1)}$. In an ideal sphere for $l=1$,

$$h_1^{(1)}(x) = -\frac{e^{ix}}{x} \left(1 + \frac{i}{x} \right). \quad (8)$$

Substituting this form of R_{kl}^{TM} into Eqs. (5) yields

$$\chi_0^{\text{TM}} = C \frac{\sqrt{2}}{2c} \frac{e^{ikr}}{r} \left(\frac{1}{kr} + \frac{i}{k^2 r^2} \right) \hat{\mathbf{e}}_0, \quad (9)$$

$$\chi_{\pm 1}^{\text{TM}} = \pm C \frac{\sqrt{2}}{c} \frac{e^{ikr}}{r} \left(i - \frac{1}{kr} - \frac{i}{k^2 r^2} \right) \hat{\mathbf{e}}_{\pm 1}. \quad (10)$$

III. DIAGONALIZATION OF THE FIELD-ATOM HAMILTONIAN

The RWA Hamiltonian of interaction [Eq. (1)] between a $j=0 \leftrightarrow j=1$ dipole transition and a triplet of effectively degenerate angular-momentum eigenmodes, $m=0, \pm 1$, $l \geq 1$, in the cases discussed above, can be diagonalized in the four-dimensional subspace of field-atom product states:

$$\begin{aligned} &|e_1; N_1 - 1, N_0, N_{-1}\rangle, \\ &|e_0; N_1, N_0 - 1, N_{-1}\rangle, \\ &|e_{-1}; N_1, N_0, N_{-1} - 1\rangle, \\ &|g; N_1, N_0, N_{-1}\rangle. \end{aligned} \quad (11a)$$

Here the relevant atomic eigenstates are $\{|e_1\rangle, |e_0\rangle, |e_{-1}\rangle, |g\rangle\}$ corresponding to the three excited states ($j=1, m_j=0, \pm 1$) and one ground state ($j=0, m_j=0$). The photon numbers in modes with $m = \pm 1, 0$, $l \geq 1$, are denoted by $N_{\pm 1}$, N_0 , respectively. We restrict here our basis to photon numbers such that

$$\sum_{m=\pm 1, 0} N_m \equiv N \geq 1, \quad (11b)$$

N being the total photon number when the atom is in the $|g\rangle$ state. We thus exclude the $|g, N=0\rangle$ state, which is uncoupled from the other states. In this basis the Hamiltonian can be expressed as

$$\hat{\mathbf{H}}^\beta = \hbar \begin{pmatrix} N\omega - \Delta & 0 & 0 & \chi_1^\beta \sqrt{N_1} \\ 0 & N\omega - \Delta & 0 & \chi_0^\beta \sqrt{N_0} \\ 0 & 0 & N\omega - \Delta & \chi_{-1}^\beta \sqrt{N_{-1}} \\ (\chi_1^\beta)^* \sqrt{N_1} & (\chi_0^\beta)^* \sqrt{N_0} & (\chi_{-1}^\beta)^* \sqrt{N_{-1}} & N\omega \end{pmatrix}, \quad (12)$$

where ω is the mode frequency and $\Delta = \omega - \omega_0$ is the detuning from the atomic resonance frequency.

Diagonalization of the matrix (12) yields the eigenfrequencies

$$E_{1,2} = \hbar(N\omega - \Delta), \quad E_{3,4} = \hbar(N\omega - \Delta/2 \pm W_N), \quad (13)$$

where, using the fact that $|\chi_1^\beta|^2 = |\chi_{-1}^\beta|^2$, we express the field-induced energy shift as

$$W_N \equiv \sqrt{(\Delta/2)^2 + N_+ |\chi_1^\beta|^2 + N_0 |\chi_0^\beta|^2}, \quad (14a)$$

with

$$N_+ \equiv N_1 + N_{-1}. \quad (14b)$$

Consistent with (11b), if $\chi_0 = 0$ (as in the TE case), then $N_+ \geq 1$, and, if both $\chi_0, \chi_1 \neq 0$ then $N = N_+ + N_0 \geq 1$. The corresponding eigenvectors are given by

$$|u_{1,2}\rangle = \begin{pmatrix} c_1 \\ c_0 \\ c_{-1} \\ 0 \end{pmatrix}, \quad (15)$$

with coefficients that satisfy the equation

$$\sum_{m=0,\pm 1} c_m \chi_m^* \sqrt{N_m} = 0 \quad (16)$$

and

$$|u_{3,4}\rangle = \frac{1}{\sqrt{2W_N^2 \pm \Delta W_N}} \begin{pmatrix} \chi_1 \sqrt{N_1} \\ \chi_0 \sqrt{N_0} \\ \chi_{-1} \sqrt{N_{-1}} \\ \Delta/2 \pm W_N \end{pmatrix}. \quad (17)$$

Equations (15) and (16) show that there are two ‘‘dark’’ (trapping) states $|u_{1,2}\rangle$ in which the atom is excited and stable against emission of the photon, because the two emission processes (with left- and right-circular photon polarizations) in these states exhibit destructive interference. The corresponding eigenvalues $E_{1,2}$ [Eq. (13)] are not affected by the field-atom interaction; i.e., the atom is essentially decoupled from the field. As is well known, in a Λ configuration there is only one dark (trapping) state.

Note that the TE case ($\chi_0^{\text{TE}} = 0$) is equivalent to the TM case with either $N_0 = 0$ or with the atom located at a χ_0^{TM} node. In the following, the indices β and j will be suppressed unless required.

IV. GENERALIZED RABI OSCILLATIONS

The eigenenergies and eigenvectors derived above allow us to calculate the time-dependent atomic transition amplitudes for a given photon number. When the atom is initially in the ground state, and the state at $t=0$ is $|g; \{N_m\} = \{N_1, N_0, N_{-1}\}\rangle$, the $|g\rangle \rightarrow |e_m\rangle$ transition amplitude has the form

$$A_{\{N_m\}}^{g \rightarrow e_m}(t) = \frac{i\chi_m \sqrt{N_m}}{W_N} e^{-i(N_m - \Delta/2)t} \sin W_N t. \quad (18a)$$

For an atom initially in the $|e_m\rangle$ state, with $\{N_m\}$ photons in the field,

$$A_{\{N_{m-1}\}}^{e_m \rightarrow g} = A_{\{N_m\}}^{*g \rightarrow e_m}(t). \quad (18b)$$

The corresponding $|g\rangle \rightarrow |e_m\rangle$ transition probabilities are

$$P_{\{N_m\}}^{g \rightarrow e_m} = N_m |\chi_m|^2 \sin^2(W_N t) / W_N^2 \quad (19a)$$

and the probability to remain in the ground state is

$$P_{\{N_m\}}^{g \rightarrow g} = 1 - \left(\sum_{m=0,\pm 1} N_m |\chi_m|^2 \right) \sin^2(W_N t) / W_N^2. \quad (19b)$$

Hence, Rabi oscillations occur with a frequency $W_N = \sqrt{(\Delta/2)^2 + |\chi|^2 N}$ that depends on the total number of photons (when the atom is in $|g\rangle$). In the TE case, $N_+ = N_1 + N_{-1}$ is the relevant photon number. The system then behaves as a two-level atom oscillating between the ground state $|g\rangle$ and the superposition of excited states $|e_+\rangle \equiv (1/\sqrt{N_+})(\sqrt{N_1}|e_1\rangle + \sqrt{N_{-1}}|e_{-1}\rangle)$, interacting effectively with a single mode having N_+ photons. The reason for this behavior is that by taking the appropriate linear combinations of the $m = \pm 1$ modes we can construct two orthogonal elliptically polarized modes, such that one mode is in a N_+ -photon state and the other is in its vacuum state. Clearly, the atom, initially in the ground state, can only exchange one *elliptically polarized* photon with the field.

Generally, for both TE and TM polarizations, the evolution of any initial superposition of $|e_m\rangle$ and $|N_m\rangle$ states can be described as the beating of oscillations with frequency W_N and population trapping at the ‘‘dark’’ states [Eqs. (15)–(17)]. The results of such beating are discussed below.

V. COLLAPSES AND REVIVALS

We wish to explore the mode interference effects in both the TE and TM cases on the collapse and revival patterns of the Rabi oscillations, obtainable for a multimode field initially in a coherent state [7]. We assume that the modes ($l, m=0$) and ($l, m=\pm 1$) of an oblate spheroid are populated by a classical beam [Fig. 1(a)].

A. The atom initially in the ground state

Assume that initially the atom is in the ground state, and the field is in the multimode coherent state $|\{\alpha_m\} = \alpha_1, \alpha_0, \alpha_{-1}\rangle$. In the photon-number basis, the initial state has the form

$$|g, \{\alpha_m\}\rangle = \prod_{m=0,\pm 1} e^{-|\alpha_m|^2/2} \sum_{N_m=0}^{\infty} \frac{\alpha_m^{N_m}}{\sqrt{N_m!}} |g, \{N_m\}\rangle. \quad (20)$$

The probability of the atom remaining in the ground state can be expressed [using Eqs. (18) and (19)] as

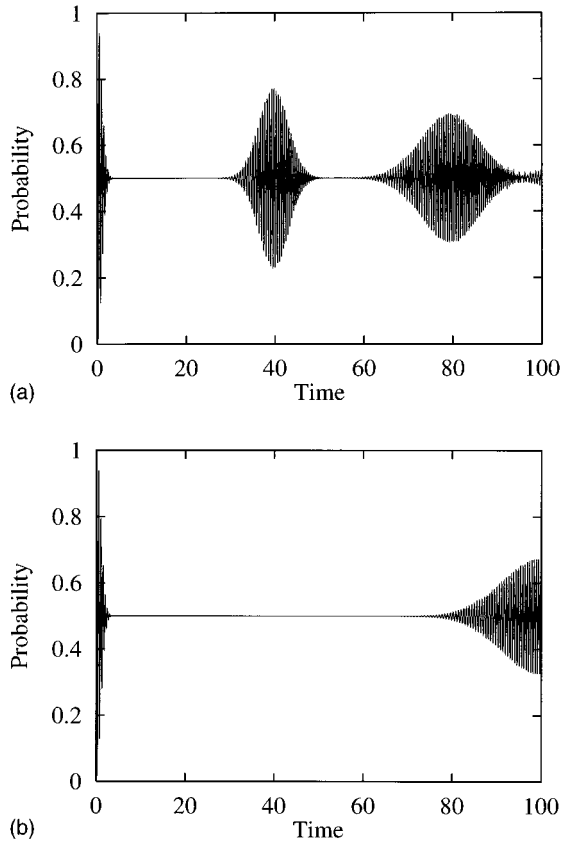


FIG. 2. The probability to remain in the initial ground state as a function of time (scaled to the inverse coupling constant) for an initial coherent-state TM-polarized field: (a) $|\alpha_+|^2 = |\alpha_0|^2 = 20$, $|\chi_0|^2 = |\chi_1|^2 = 1$. (b) Same α_+ , α_0 ; $|\chi_0|^2 = 0.8$, $|\chi_1|^2 = 1.2$. Note the drastic change in the revival patterns.

$$P_{\{a_m\}}^{g \rightarrow g}(t) = e^{-|\alpha_+|^2 - |\alpha_0|^2} \sum_{N_+, N_0} \frac{|\alpha_0|^{2N_0} |\alpha_+|^{2N_+}}{N_0! N_+!} \times \left(1 - \frac{|\chi_1|^2 N_+ + |\chi_0|^2 N_0}{\bar{W}_N^2} \sin^2 \bar{W}_N t \right), \quad (21)$$

where $|\alpha_+|^2 = |\alpha_1|^2 + |\alpha_{-1}|^2$, and \bar{W}_N is defined in Eq. (14).

In the case of coherent TE-mode excitation, (21) can be simplified (substituting $\chi_0 = 0$ and $\bar{W}_N = \bar{W}_{N_+}$) as follows:

$$P_{\alpha_1 \alpha_{-1}}^{g \rightarrow g}(t) = e^{-|\alpha_+|^2} \sum_{N_+} \frac{|\alpha_+|^{2N_+}}{N_+!} \times \left(1 - \frac{|\chi_1|^2 N_+}{\bar{W}_{N_+}^2} \sin^2 \bar{W}_{N_+} t \right). \quad (22)$$

This expression exhibits the usual collapse and revival behavior in the linear combination of the right- and left-handed circular-polarized coherent states. In this case, the atom basically interacts with one elliptically polarized coherent state. The dark state for this case corresponds to atomic excitation by photons with the orthogonal elliptical polarization.

New phenomena are predicted in the case of coherent TM-mode excitation. The numerical plots of Eq. (21) for this case (Fig. 2) reveal unusual features, i.e., suppression and/or delay of the revivals. In order to gain insight into these fea-

tures, we use the following *crude* approximation for the case of resonance, $\Delta = 0$, and large average photon numbers $|\alpha_+|^2, |\alpha_0|^2 \gg 1$. We expand the square root in \bar{W}_N up to the linear term

$$\sqrt{|\chi_0^\beta|^2 N_0 + |\chi_1^\beta|^2 N_+} \approx \frac{1}{2} \sqrt{|\chi_0^\beta|^2 |\alpha_0|^2 + |\chi_1^\beta|^2 |\alpha_+|^2} + \frac{|\chi_0^\beta|^2 N_0 + |\chi_1^\beta|^2 N_+}{2 \sqrt{|\chi_0^\beta|^2 |\alpha_0|^2 + |\chi_1^\beta|^2 |\alpha_+|^2}}. \quad (23)$$

This expansion is justified since the Poisson distributions are centered around $|\alpha_0|^2$ or $|\alpha_+|^2$ over a width of the order of $|\alpha_0|$ or $|\alpha_+|$, respectively. This approximation allows one to perform both sums in Eq. (21) analytically, yielding

$$P_{\{a_m\}}^{g \rightarrow g}(t) \approx \frac{1}{2} \left[1 + \exp \left(-2|\alpha_+|^2 \sin^2 \frac{|\chi_1^\beta|^2 t}{2\bar{W}} - 2|\alpha_0|^2 \times \sin^2 \frac{|\chi_0^\beta|^2 t}{2\bar{W}} \right) \cos \left(\bar{W}t + |\alpha_0|^2 \sin \frac{|\chi_0^\beta|^2 t}{\bar{W}} + |\alpha_+|^2 \sin \frac{|\chi_1^\beta|^2 t}{\bar{W}} \right) \right], \quad (24)$$

where $\bar{W} = \sqrt{|\chi_1 \alpha_+|^2 + |\chi_0 \alpha_0|^2}$. The terms $\exp(-2|\alpha_+|^2 \sin^2 |\chi_1|^2 t / 2\bar{W})$ and $\exp(-2|\alpha_0|^2 \sin^2 |\chi_0|^2 t / 2\bar{W})$ can be regarded as envelopes for the Rabi oscillations with the average frequency \bar{W} . Revivals occur when *both* envelopes differ noticeably from zero, i.e., around the times given by

$$\frac{|\chi_1|^2 t_{\nu_1}}{2\bar{W}} = \nu_1 \pi, \quad \frac{|\chi_0|^2 t_{\nu_0}}{2\bar{W}} = \nu_0 \pi. \quad (25)$$

Thus the condition for the first revival takes the form $t_{\nu_0} = t_{\nu_1}$ for the smallest integer numbers ν_0 and ν_1 such that $\nu_0/\nu_1 = |\chi_0|^2/|\chi_1|^2$. In general the required integers can be much larger than 1, in which case the first revival is effectively delayed or suppressed.

Of course, the above analysis is oversimplified: (i) partial overlap of the nonzero parts of the envelopes is sufficient to produce some remnant of a revival; (ii) expansions (23) and (24) are known to be inadequate for the subsequent revivals [22]. Nevertheless, it yields the correct prediction that an appropriate choice of the ratio $|\chi_0|^2/|\chi_1|^2$ allows one to *suppress the first revival noticeably*, as shown in Fig. 2(b), which presents the ground-state probability calculated numerically from Eq. (21). In both cases, Figs. 2(a) and 2(b), the average numbers of photons, as well as the Rabi frequencies \bar{W} are the same. The only difference is the ratio $|\chi_0|^2/|\chi_1|^2$, which is equal to 1 for the upper plot and 2/3 for the lower plot. Suppression of the first revival is clearly visible.

We next consider the probability of the initial state (20) to yield $|g\rangle \rightarrow |e_m\rangle$ transitions. It is convenient to consider the combined population of $|e_1\rangle$ and $|e_{-1}\rangle$:

$$P_{\{\alpha_m\}}^{g \rightarrow e_1}(t) + P_{\{\alpha_m\}}^{g \rightarrow e_{-1}}(t) = e^{-|\alpha_+|^2 - |\alpha_0|^2} \sum_{N_+, N_0} \frac{|\alpha_0|^{2N_0} |\alpha_+|^{2N_+}}{N_0! N_+!} \times \frac{|\chi_1|^2}{W_N^2} N_+ \sin^2(W_N t), \quad (26)$$

whereas the population of the excited $|e_0\rangle$ sublevel is

$$P_{\{\alpha_m\}}^{g \rightarrow e_0}(t) = e^{-|\alpha_+|^2 - |\alpha_0|^2} \sum_{N_+, N_0} \frac{|\alpha_0|^{2N_0} |\alpha_+|^{2N_+}}{N_0! N_+!} \times \frac{|\chi_0|^2 N_0}{W_N^2} \sin^2(W_N t). \quad (27)$$

Equations (26) and (27) differ only by one factor in the summation, $|\chi_1|^2 N_+ / W_{N_+, N_0}^2$ as compared to $|\chi_0|^2 N_0 / W_N^2$. Let us rewrite these factors as

$$\frac{|\chi_m|^2 N_m}{W_N^2} = \left(\frac{|\chi_m|^2 N_m}{|\chi_1|^2 N_+ + |\chi_0|^2 N_0} \right) \left(\frac{|\chi_1|^2 N_+ + |\chi_0|^2 N_0}{W_N^2} \right) \quad (28)$$

and take the values of the first fraction that make the dominant contribution to the sum, at $N_m \approx |\alpha_m|^2$. Then we obtain

$$P_{\{\alpha_m\}}^{g \rightarrow e_1}(t) + P_{\{\alpha_m\}}^{g \rightarrow e_{-1}}(t) \approx \frac{|\chi_1|^2 \alpha_+|^2}{|\chi_1 \alpha_+|^2 + |\chi_0 \alpha_0|^2} [1 - P_{\{\alpha_m\}}^{g \rightarrow g}(t)], \quad (29)$$

$$P_{\{\alpha_m\}}^{g \rightarrow e_0}(t) \approx \frac{|\chi_0 \alpha_0|^2}{|\chi_1 \alpha_+|^2 + |\chi_0 \alpha_0|^2} [1 - P_{\{\alpha_m\}}^{g \rightarrow g}(t)]. \quad (30)$$

Thus, under this approximation, the occupations of the upper levels are equal to $1 - P_{\{\alpha_m\}}^{g \rightarrow g}(t)$, reduced by the fractional weight of the squared coupling constant times the average photon number in the pertinent mode.

This simplified analysis is confirmed by numerical calculations of the excited-level populations shown in Figs. 3 and 4 for different average photon numbers and coupling constants. It is easily seen that the *time of the first revival depends only on the ratio* of $|\chi_0|^2 / |\chi_1|^2$. The products $|\chi_0 \alpha_0|^2$ and $|\chi_1 \alpha_+|^2$ determine which atomic sublevel is more populated by the interaction with the field.

B. Initially excited states

An initial superposition of excited-state sublevels and multimode coherent states $\sum_m c_m |e_m, \{\alpha_m\}\rangle$ yields the following probability of occupying the ground state:

$$P_{\{\alpha_m\}}^g = \sum_{N_0, N_{\pm 1}} \left(\prod_m e^{-|\alpha_m|^2} \right) \sum_m \frac{|\alpha_m|^{2N_m}}{N_m!} \times \left| \sum_m \frac{c_m \sqrt{N_m}}{\alpha_m} A_{\{N_m\}}^{e_m \rightarrow g} \right|^2. \quad (31)$$

On substituting the $A_{\{N_m\}}^{e_m \rightarrow g}$ amplitudes [Eq. (18b)] we find that

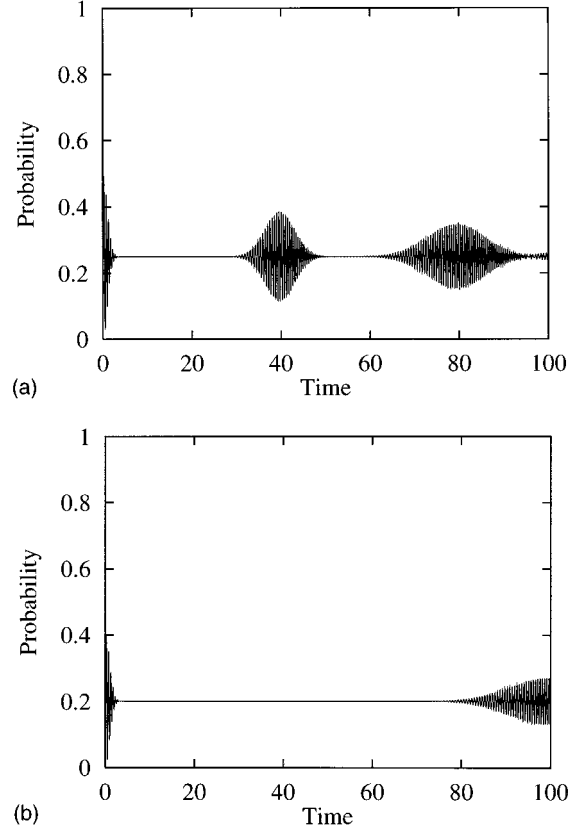


FIG. 3. Population of the excited state $|e_0\rangle$ as a function of time (same units) for the same initial conditions as in Fig. 2: (a) $|\chi_0|^2 = |\chi_1|^2 = 1$, (b) $|\chi_0|^2 = 0.8$, $|\chi_1|^2 = 1.2$. The revival patterns are qualitatively similar to Fig. 2.

$$\sum_m c_m \frac{\sqrt{N_m}}{\alpha_m} A_{\{N_m\}}^{e_m \rightarrow g} = \frac{1}{W_N^2} \left| \sum_m (-1)^m c_m \frac{\chi_m^*}{\alpha_m} N_m \right|^2. \quad (32)$$

As before, we estimate the sum in (32) by setting $N_m \approx |\alpha_m|^2$. In this approximation, the trapping condition $P_{\{\alpha_m\}}^g \approx 0$ for the initial excited-state superposition amounts to

$$\sum_m (-1)^m c_m \chi_m^* \alpha_m^* \approx 0. \quad (33)$$

Equation (33) defines the quasiclassical ‘‘dark’’ (trapping) states, for which the *energy exchange with the coherent field is suppressed*. This condition is in reasonable agreement with the numerical plots of the energy exchange (Fig. 5).

VI. DISCUSSION

We have treated the resonant nondissipative coupling of an atom with a $j=0 \leftrightarrow j=1$ dipole transition to a near-spherical (spheroidal) TE or TM polarized field by taking account of the degeneracy of atomic levels and low- m ($m=0, \pm 1$) field modes. The following results have been obtained from this treatment: (a) A photon with the suitable (‘‘active’’) elliptic polarization can produce sinusoidal Rabi oscillations between $|g\rangle$ and a superposition of degenerate excited states. Exchange of the orthogonally polarized

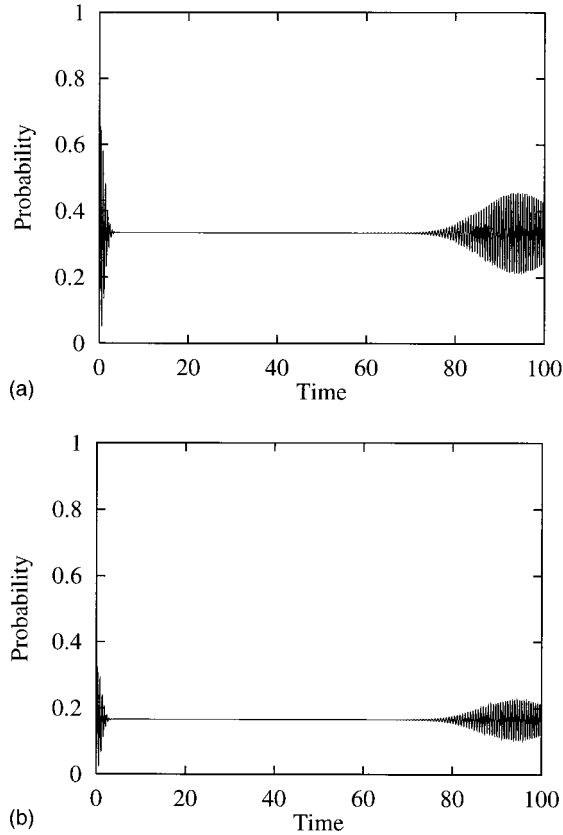


FIG. 4. Excited-state populations as a function of time (same units) for an atom initially in the ground state and an initial coherent-state TM polarized field with $|\alpha_+|^2=10$, $|\alpha_0|^2=30$, $|\chi_0|^2=0.8$, $|\chi_1|^2=1.2$: (a) population of $|e_0\rangle$; (b) combined populations of $|e_1\rangle$ and $|e_{-1}\rangle$. The revival pattern is as in Figs. (2b) and (3b).

(“dark” polarization) photon with this superposition is forbidden by the population trapping condition. The active and “dark” elliptic polarizations are *controllable* by the atomic distance from the center and the l number of the modes, which determine the coupling constants $\chi_m^\beta(r)$. (b) Population-trapping (energy-exchange suppression) effects are obtainable for elliptically polarized quasiclassical coherent fields, which are also controllable by the factors mentioned above. (c) The timing and strength of the atomic population revivals is controllable by the ratio of the squared coupling constants to the orthogonally polarized modes, $|\chi_0(r)|^2/|\chi_1(r)|^2$.

The understanding acquired here of the factors controlling the energy exchange with the field and the atomic-state population can be used for preparation of nonclassical states of the field in a dielectric microsphere. This can be achieved

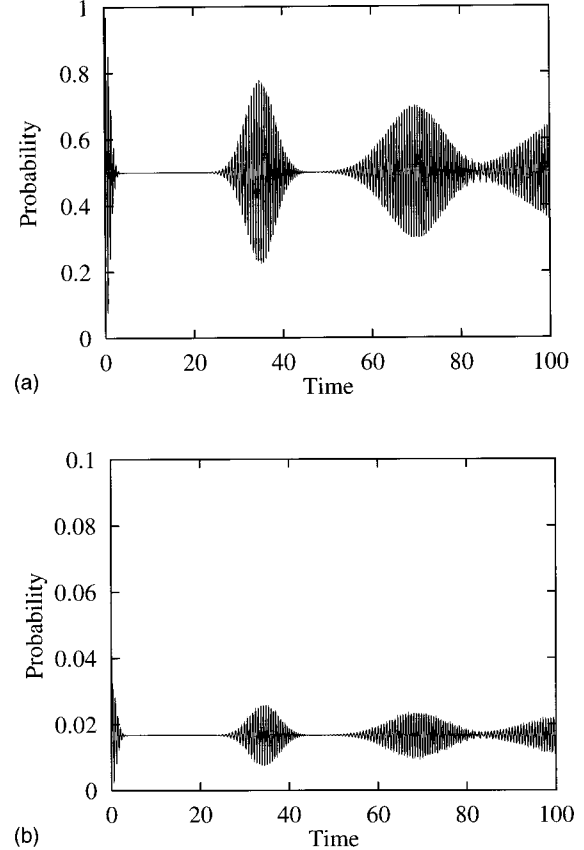


FIG. 5. Ground-state population as a function of time (same units) for initially excited atom and TM-polarized field in the coherent state, with $\alpha_1=\alpha_0=\alpha_{-1}=\sqrt{10}$ and $-\chi_1=\chi_0=\chi_{-1}=1$: (a) initial excited sublevel amplitudes $c_1=c_0=c_{-1}=1/\sqrt{3}$, (b) $c_0;c_1=-c_{-1}=1/\sqrt{2}$. Note the different scales of revival patterns.

by resonant interaction with surface-adsorbed molecules, or with cold atoms orbiting the microsphere under the influence of another off-resonant field. Finally, we have discussed the influence of weak oblateness of the sphere, and identified the conditions under which mode degeneracy effects would still be observable.

ACKNOWLEDGMENTS

D.L. and G.K. acknowledge the partial support of the Israel-Netherlands Researchers Exchange Programme. G.K. acknowledges the support of the TMR Research Network No. ERB 4061 PL 95-1021. K.B. acknowledges support of the TEMPUS program JEP-04329-94 at the Vrije Universiteit, Amsterdam.

[1] G. Rempe, H. Walther, and N. Klein, *Phys. Rev. Lett.* **58**, 353 (1987).
 [2] M. G. Raizen *et al.*, *Phys. Rev. Lett.* **63**, 240 (1989).
 [3] R. J. Thompson, G. Rempe, and H. J. Kimble, *ibid.* **68**, 1132 (1992).

[4] D. Meschede, *Phys. Rep.* **211**, 201 (1992).
 [5] E. A. Hinds, *Adv. At. Mol. Opt. Phys.* **28**, 237 (1990).
 [6] J. Jacobson *et al.*, *Phys. Rev. A* **51**, 2542 (1995).
 [7] H. I. Yoo and J. H. Eberly, *Phys. Rep.* **118**, 239 (1985).
 [8] J. H. Eberly, N. B. Narozhny, and J. J. Sanchez-Mondragon,

- Phys. Rev. Lett. **44**, 1323 (1980).
- [9] J. Krause, M. O. Scully, T. Walther, and H. Walther, Phys. Rev. A **39**, 1915 (1989).
- [10] P. Meystre, Prog. Opt. **30**, 263 (1992).
- [11] B. M. Garraway, B. Sherman, H. Moya-Cessa, P. L. Knight, and G. Kurizki, Phys. Rev. A **49**, 535 (1994).
- [12] K. Vogel, V. M. Akulin, and W. P. Schleich, Phys. Rev. Lett. **71**, 1816 (1993).
- [13] S.-C. Gou, Phys. Rev. A **40**, 5116 (1989); C. C. Gerry and J. H. Eberly, *ibid.* **42**, 6805 (1990); D. H. Cardimona *et al.*, *ibid.* **43**, 3710 (1991).
- [14] (a) W. Barber and R. K. Chang, *Optical Effects Associated with Small Particles* (World Scientific, Singapore, 1988); (b) S. C. Ching, M. M. Lai, and K. Young, J. Opt. Soc. Am. B **4**, 2004 (1987).
- [15] B. Sherman and G. Kurizki, Phys. Rev. A **45**, R7674 (1992).
- [16] H. Mabuchi and H. J. Kimble, Opt. Lett. **19**, 749 (1994).
- [17] G. Kurizki and A. Nitzan, Phys. Rev. A **38**, 267 (1988).
- [18] S. C. Hill and R. E. Benner, J. Opt. Soc. Am. B **3**, 1509 (1986).
- [19] S. C. Ching, H. M. Lai, and K. Young, *ibid.* **4**, 1995 (1987); **4**, 2004 (1987).
- [20] L. Wang, R. R. Puri, and J. H. Eberly, Phys. Rev. A **46**, 7192 (1992); L. Wang and J. H. Eberly, *ibid.* **47**, 4248 (1993).
- [21] H. M. Lai *et al.*, Phys. Rev. A **41**, 5187 (1990).
- [22] I. Sh. Averbukh and N. F. Perelman, Usp. Fiz. Nauk **161**, 41 (1991) [Sov. Phys. Usp. **34**, 572 (1991).]